

Breast percent density estimation from 3D reconstructed digital breast tomosynthesis images

Predrag R. Bakic^{*}, Despina Kontos, Ann-Katherine Carton, and Andrew D.A. Maidment
Department of Radiology, University of Pennsylvania,
3400 Spruce Street, Philadelphia, PA 19104

ABSTRACT

Breast density is an independent factor of breast cancer risk. In mammograms breast density is quantitatively measured as percent density (PD), the percentage of dense (non-fatty) tissue. To date, clinical estimates of PD have varied significantly, in part due to the projective nature of mammography. Digital breast tomosynthesis (DBT) is a 3D imaging modality in which cross-sectional images are reconstructed from a small number of projections acquired at different x-ray tube angles. Preliminary studies suggest that DBT is superior to mammography in tissue visualization, since superimposed anatomical structures present in mammograms are filtered out. We hypothesize that DBT could also provide a more accurate breast density estimation. In this paper, we propose to estimate PD from reconstructed DBT images using a semi-automated thresholding technique. Preprocessing is performed to exclude the image background and the area of the pectoral muscle. Threshold values are selected manually from a small number of reconstructed slices; a combination of these thresholds is applied to each slice throughout the entire reconstructed DBT volume. The proposed method was validated using images of women with recently detected abnormalities or with biopsy-proven cancers; only contralateral breasts were analyzed. The Pearson correlation and kappa coefficients between the breast density estimates from DBT and the corresponding digital mammogram indicate moderate agreement between the two modalities, comparable with our previous results from 2D DBT projections. Percent density appears to be a robust measure for breast density assessment in both 2D and 3D x-ray breast imaging modalities using thresholding.

Keywords: Imaging of the breast, Tomosynthesis, Algorithms.

1. INTRODUCTION

Mammographic breast density is an independent factor of breast cancer risk.¹ Excluding genotype, breast density is the strongest correlate with the relative risk of developing breast cancer. Studies have shown that women with very dense breasts have a 4- to 6-fold increase in breast cancer relative risk compared to women with the least dense breasts, as measured mammographically.² In mammograms, breast density is quantitatively measured as percent density (PD), the percentage of non-fatty (dense) tissue. PD is calculated by thresholding the pixel grey-level values signal intensity in the mammograms.

Digital breast tomosynthesis (DBT) is an emerging x-ray imaging technique that provides a 3D visualization of the breast tissue; cross-sectional images are reconstructed from a small number of source projection images that are acquired over a limited angular range of the x-ray tube position.³ Preliminary studies have shown that DBT is superior to mammography in visualization and characterization of breast tissue since the superimposed anatomical structures present in mammograms are nearly filtered out.⁴

Breast density can be calculated from DBT; it can be calculated either from the projection images or from the reconstructed tomographic images. The DBT projection images are similar to low-dose mammograms, and, thus, breast density can be calculated in a similar way to mammograms. In our previous work, we calculated breast density from the projection data, and observed high similarity with mammographic estimate, PD_M .⁵ However, such an approach to breast density estimation does not use any additional 3D information available from DBT.

^{*} Predrag.Bakic@uphs.upenn.edu; Phone: 215 746 8758; Fax: 215 746 8764

Due to their 3D nature, reconstructed DBT images could provide a more realistic estimation of breast density. Breast density can be estimated from each of the individual reconstructed slices using the thresholding methods for PD_M estimation. By combining the slice-wise estimates, a volumetric, 3D breast density estimate, $PD_{T,3D}$, can be obtained. In this paper, we present the results of the $PD_{T,3D}$ estimation from reconstructed DBT images, using an extension of the thresholding-based method for PD_M estimation. $PD_{T,3D}$ estimates are compared to PD_M .

2. MATERIALS AND METHODS

2.1 Patient population

DBT image data were retrospectively collected from a clinical multimodality imaging study in our department (NIH R01 CA85484-01A2) in which bilateral DBT, digital mammography (DM), MRI, ultrasound, and PET of the same women were performed the same day. This study included women with recently detected abnormalities or with biopsy proven cancers. For our study, only breasts contralateral to abnormalities were considered. Of 51 women who presented for a DBT exam, we selected 35. Sixteen women were excluded due to the existence or suspicion of bilateral cancer, or due to incomplete visualization of the breast tissue which precluded the breast density estimation.

2.2 Acquisition and processing of clinical images

Imaging was performed with a GE Senographe 2000D FFDM system (General Electric Medical Systems, Milwaukee, WI), modified to allow DBT. For the DBT exam, the breast was positioned in MLO position and immobilized with light compression (4 to 6 daN). The breast support table did not contain an anti-scatter grid. Each DBT image data set consists of nine projection images acquired in 6.25-degree increments over a 50 degree arc. The pixel pitch was 100 μm . The radiation dose for each tomosynthesis data set was similar to the mean glandular dose used for a standard 2-view mammographic exam.⁵ A custom filtered-backprojection method was used to reconstruct DBT tomographic planes in 1 mm increments with 0.22 mm in-plane resolution. A volume of interest of $20.5 \times 20.5 \times T \text{ cm}^3$ was reconstructed, where T was equal to the thickness of the breast as measured by the compression device and recorded in the source image DICOM header. For the DM exam, the breast was positioned in both MLO and CC positions, each mammographic projection was acquired with an anti-scatter grid, and a 100 μm spatial resolution.

2.3 Breast density estimation from DM and DBT images

For PD_M estimation, the Cumulus 4.0 software package developed at the University of Toronto⁶ was used; Cumulus has been validated in many studies.⁷⁻¹⁰ Cumulus is based on manual exclusion of the pectoral muscle and interactive selection of thresholds for segmenting the breast outline and the regions of dense tissue. PD_M is computed as the ratio of the area corresponding to the dense tissue in a mammogram and the total mammographic breast area. In this paper, we computed PD_M on MLO mammographic views, as the DBT images were acquired with the breast positioned for the MLO view.

For the volumetric, $PD_{T,3D}$, estimation we propose a semi-automated threshold-based method. Cumulus was used to analyze a small number of tomographic slices to account for per-slice threshold variations within the same breast volume. For each of the analyzed slices, the pectoral muscle border was approximated by a straight line, and its intercepts with the horizontal and vertical slice edge were recorded. The average values of the intercepts were used to define a 3D pectoral mask applied to all the reconstructed slices of the DBT image. Two threshold values were selected manually from the analyzed reconstructed slices: one for the breast outline, and another for segmenting the dense tissue area. In this paper we analyzed three slices corresponding to 30th, 50th, and 70th percentile of the total number of reconstructed slices. A combination of the manually selected thresholds is applied to all the tomographic slices of each DBT image set; in this paper we used the average value of the selected thresholds. $PD_{T,3D}$ is estimated as the ratio between the number of voxels containing dense breast tissue, and the total number of voxels in the entire breast volume. In addition to volumetric $PD_{T,3D}$ estimation, we also estimated breast density from individual reconstructed slices, $PD_{T,slices}$, as the ratio between the number of dense tissue pixels and all breast pixels within the tomographic slice.

Due to artifacts in the DBT reconstruction, portions of the background (non-breast) have digital values above the threshold for segmentation of the breast border, which could cause an error in density estimation (see Figure 1 left). Most of those artifacts were eliminated by setting the pixel values to zero in the area outside the breast.

2.4 Statistical comparison between $PD_{T,3D}$ and PD_M estimates

We analyzed the agreement between $PD_{T,3D}$ and PD_M was performed by computing the Pearson correlation coefficient, r , defined as:

$$r = \frac{\sum (PD_M \cdot PD_{T,3D})}{\sqrt{(\sum PD_M^2) \cdot (\sum PD_{T,3D}^2)}} \quad (1).$$

In addition, we categorized $PD_{T,3D}$ and PD_M values into 6 classes of density,[†] as proposed by Byng *et al.*,⁶ and analyzed their agreement using kappa statistics. The kappa coefficient, κ , describes the agreement between categorical results of repeated diagnostic ratings performed by the same or different observers, while taking into account only the agreement beyond that expected by chance:¹¹

$$\kappa = \frac{P_0 - P_C}{1 - P_C}, \quad (2)$$

where P_0 and P_C represent the proportion of observed agreements and the proportion of agreements expected by chance, respectively. When the rating results are presented by a multi-category ordinal scale, the proportions of agreements used to compute κ are usually weighted to reflect different degrees of disagreement between larger and smaller rating differences;¹¹ quadratic weights were used in our study.

3. RESULTS

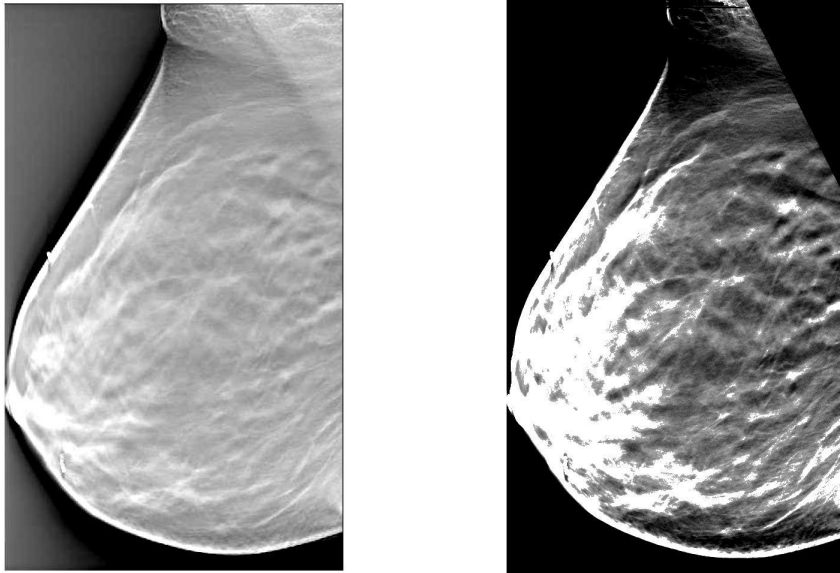


Figure 1: Examples of an original reconstructed DBT slice (left) and the same slice after the segmentation of the breast background and the dense tissue regions (right). Segmented slices are used in $PD_{T,3D}$ estimation.

Figure 1 illustrates a reconstructed DBT slice before and after the segmentation of the breast outline and the region of dense tissue, as described in Section 2.3. Segmented slices (right) are used in $PD_{T,3D}$ estimation. For the breast shown in Figure 1, $PD_{T,3D} = 22\%$.

[†] The 6 classes of PD were defined as:⁶ (i) $PD = 0\%$; (ii) $0\% < PD \leq 10\%$; (iii) $10\% < PD \leq 25\%$; (iv) $25\% < PD \leq 50\%$; (v) $50\% < PD \leq 75\%$; and (vi) $PD \leq 75\%$.

Figure 2 left shows the distributions of $PD_{T,3D}$ and PD_M values. Figure 2 right shows a scatter-plot of $PD_{T,3D}$ vs. PD_M . For 35 analyzed breasts an average value and standard deviation were calculated. For the DBT method, $PD_{T,3D} = 28 \pm 19\%$, while for the mammographic method $PD_M = 36 \pm 20\%$. The Pearson correlation coefficient between $PD_{T,3D}$ and PD_M was equal to $r = 0.76$ and the quadratic weighted kappa coefficient was equal to $\kappa = 0.56$.

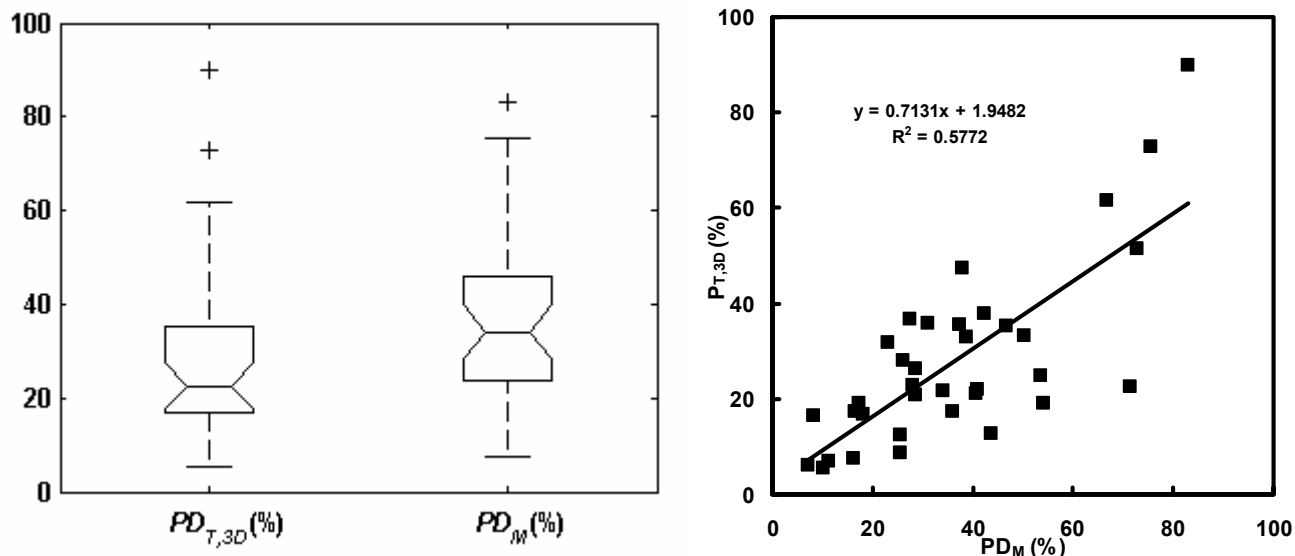


Figure 2. Box-plot (left) and scatter-plot (right) of the $PD_{T,3D}$ and PD_M values.

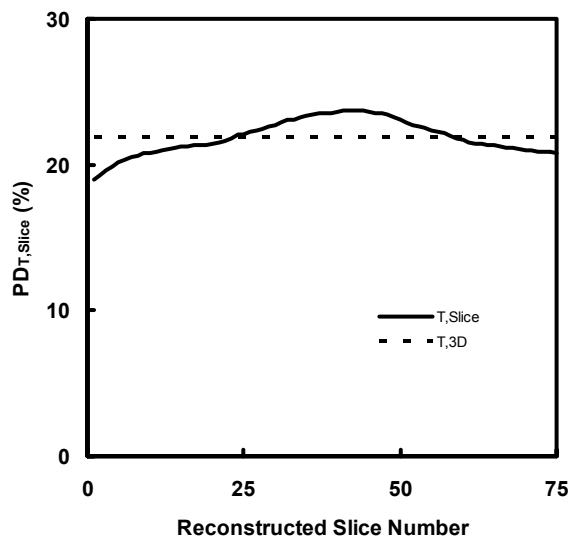


Figure 3. Estimates of $PD_{T, Slice}$ and $PD_{T, 3D}$ computed for the breast shown in Figure 1.

Figure 3 shows all $PD_{T, Slice}$ estimates (solid line) of the breast shown in Figure 1. $PD_{T, Slice}$ values were computed as described in Section 2.3. The average value and the standard deviation of the slice-wise breast density estimates for this breast were equal to $PD_{T, Slice} = 22 \pm 2\%$.

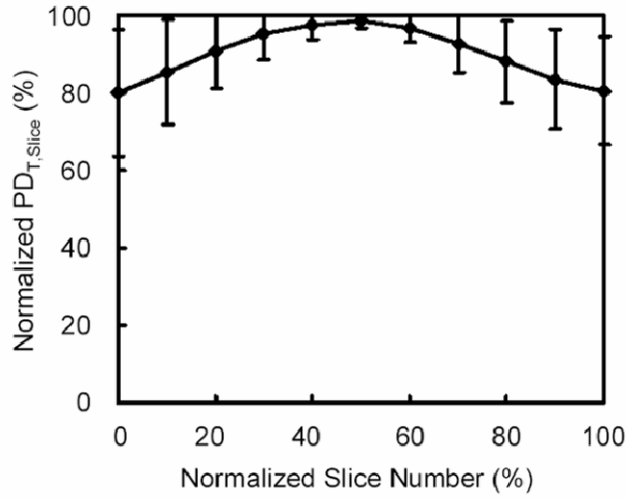


Figure 4. The normalized slice-wise breast density estimate, $PD_{T,Slice}^{norm}$ averaged over all 35 analyzed breasts; error bars indicate one standard deviation.

To compare the variation of $PD_{T,Slice}$ throughout the reconstructed breast volume (shown in Figure 3,) for all the analyzed breasts, normalized slice-wise estimates were computed as:

$$PD_{T,Slice}^{norm}(i_{\%}) = \frac{PD_{T,Slice}(i_{\%})}{[PD_{T,Slice}(i_{\%})]_{max}}; \quad i_{\%} = \frac{i}{i_{max}} \times 100\%, \quad (3)$$

where $[PD_{T,Slice}(i_{\%})]_{max}$ represents the maximum $PD_{T,Slice}$ from all the reconstructed DBT slices, i is the slice number, i_{max} is the maximum slice number corresponding to the breast thickness, and $i_{\%}$ is the normalized slice number equal to the percent of the breast thickness. Figure 4 shows the $PD_{T,Slice}^{norm}$ values at different positions within the breast, averaged over all 35 breasts; error bars indicate one standard deviation.

4. DISCUSSION

Our results from Figure 2 indicate moderate[‡] agreement between $PD_{T,3D}$ and PD_M ($r = 0.76$ and $\kappa = 0.56$), based on the standards for kappa statistics strength.¹² On average, $PD_{T,3D}$ values were lower than PD_M values of the same breast; the average $PD_{T,3D}$ and PD_M for 35 analyzed breasts were equal to 28% and 36%. This agreement is comparable with that observed in our previous study of PD_M vs. breast density estimated from the central DBT projections.⁵ That study yielded slightly stronger agreement ($r = 0.86$ and $\kappa = 0.78$). We also observed relatively small changes in PD with projection angle variation (standard deviation=1-7%).

Results from our current and previous studies of tomosynthetic breast density, although drawn from a relatively small sample size, indicate a substantial agreement between PD_M and the estimates from DBT projections or reconstructed data of the same breast. The observed agreement suggests that percent density appears to be a breast density measure robust for assessment from 2D and 3D x-ray breast imaging modalities using thresholding approach.

[‡] Standards for kappa statistics strengths, proposed by Landis and Koch¹¹ are: $\kappa \leq 0$: poor; $0.01 \leq \kappa \leq 0.20$: slight; $0.21 \leq \kappa \leq 0.40$: fair; $0.41 \leq \kappa \leq 0.60$: moderate; $0.61 \leq \kappa \leq 0.80$: substantial, and $0.81 \leq \kappa \leq 1$: almost perfect.

Figure 3 shows variation in $PD_{T, Slice}$ throughout the reconstructed breast volume. The average value of $PD_{T, Slice}$ was very close to the corresponding $PD_{T, 3D}$; their difference was less than 1%. Figure 4 shows relatively large values of the normalized $PD_{T, Slice}^{norm}$, computed by Equation (3), in practically all the slices throughout the reconstructed volume. This corresponds to relatively large regions of dense tissue segmented in the reconstructed slices, even near the breast surface. Anatomically, no significant amount of dense tissue is found near the breast surface; instead this part of the breast is occupied by subcutaneous fat. Figure 5 shows the segmented dense tissue in the central reconstructed DBT slice (lower left) and in a slice near the surface (lower right) of the same breast, obtained by the thresholding method proposed in this paper. These segmentation results correspond to $PD_M = 41\%$, and $PD_{T, Slice} = 24\%$ and 19% for the central slice and the slice near the breast surface, respectively. The corresponding $PD_{T, 3D} = 22\%$ and the average $PD_{T, Slice}$ was equal to 22% .

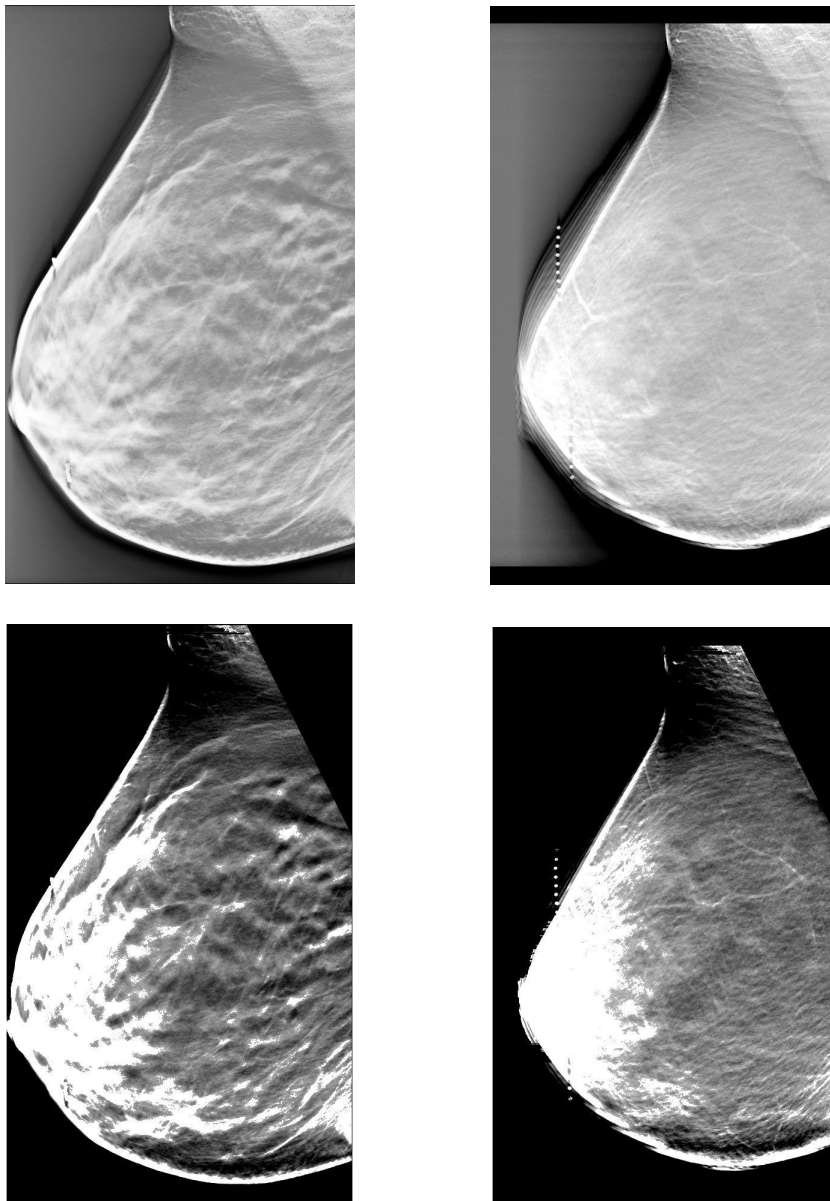


Figure 5. The central reconstructed DBT slice of the breast from Figure 1, shown before (upper left) and after (lower left) segmentation of dense tissue using the thresholding method for volumetric $PD_{T, 3D}$ estimation proposed in this paper. A reconstructed DBT slice near the surface of the same breast, shown before (upper right) and after (lower right) application of the proposed thresholding, showing a large region of out-of-focus density. The out-of-focus density causes segmentation errors in the parts of the breast where no dense tissue exists anatomically, (e.g., near the breast surface).

The observed segmentation results are the effect of the out-of-focus dense regions, due to the small number of projection images and the narrow angular range used in DBT reconstruction.¹³ Reconstructed DBT images are not truly tomographic; instead, they represent a mixture of contributions from both in- and out-of-focus objects. Regions of dense tissue in the breast usually represent large, low spatial frequency objects, and their out-of-focus contributions appear in many reconstructed DBT slices. In parts of the breast with large amounts of dense tissue (*e.g.*, the center of the breast volume) the effect of out-of-focus densities is the least noticeable. This is consistent with our results of applying Cumulus to the central reconstructed DBT slices; we observed substantial agreement between such obtained $PD_{T,Slice}$ and the corresponding PD_M ($r = 0.88$, and $k = 0.79$).

On the other hand, the effect of the out-of-focus densities is the most evident in parts of the breast in which no dense tissue exists anatomically, *e.g.*, near the breast surface (Figure 5), where they may cause errors in thresholding-based segmentation. The observed effects suggest that a direct thresholding approach is not sufficient for an accurate segmentation of the breast dense regions from currently available DBT data. Accurate assessment of the spatial and volumetric distribution of dense tissue is of interest due to the recent evidence of spatial correlation between the sites of breast cancer occurrence and regions of breast density¹⁴ and the suggestion that cancer risk is related to the actual volumetric distribution and amount of glandular tissue rather than the projected 2D area only.¹⁵ Accurate segmentation of reconstructed DBT images might require further technological improvements in clinical image acquisition, DBT image reconstruction, and reconstructed image segmentation either based on intensity thresholding techniques, as described in this paper, or on other DBT image properties, *e.g.*, fuzzy-connectedness,¹⁶ morphology, or texture.¹⁷

5. CONCLUSIONS

We proposed and evaluated a semi-automated threshold-based method to estimate 3D PD from reconstructed DBT images. The mammographic PD estimation software Cumulus was applied to only three reconstructed slices of each DBT set to manually select threshold values for segmenting the breast outline and dense tissue area. The pectoral muscle area in each reconstructed slice was excluded from the analysis using the average linear approximation of the muscle border from this limited number of slices. The average value of the manually selected thresholds is applied to all the tomographic slices of each DBT image. A correlation of 0.76 and kappa coefficient of 0.56 were observed between mammographic and DBT volumetric PD estimates; this result is comparable with our previous 2D analysis of DBT projections and central reconstructed images. Based on these agreements, PD showed robustness in assessing breast density by thresholding, in both 2D and 3D x-ray breast images. We noticed the effect of out-of-focus densities, caused by the limited number of projection images used in DBT reconstruction. The out-of-focus densities may cause errors in thresholding based segmentation, especially in parts of the breast with no dense tissue.

ACKNOWLEDGMENT

This work was supported by Susan G. Komen Breast Cancer Foundation Research Grant BCTR133506, by the Siemens/Radiological Society of North America (RSNA) Research Fellow Grant RF0707, and by National Institutes of Health/National Cancer Institute Program Project Grant P01-CA85484.

REFERENCES

1. Martin LJ, Boyd NF. Potential mechanisms of breast cancer risk associated with mamographic density: hypotheses based on epidemiological evidence. *Breast Cancer Research*. 2008;10(1).
2. Boyd NF, Lockwood GA, Martin LJ, Byng JW, Yaffe MJ, Trichler DL. Mammographic density as a marker of susceptibility to breast cancer: a hypothesis. *LARC Scientific Publications*. 2001;154:163-169.
3. Niklason LT, Christian BT, Niklason LE, et al. Digital tomosynthesis in breast imaging. *Radiology*. 1997;205(2):399-406.

4. Rafferty E, Niklason L, Halpern E, Sumkin J, Park JM, Poplack S. Assessing Radiologist Performance Using Combined Full-Field Digital Mammography and Breast Tomosynthesis Versus Full-Field Digital Mammography Alone: Results of a Multi-Center, Multi-Reader Trial Paper presented at: RSNA 2007, 2007; Chicago, IL.
5. Bakic PR, Kontos D, Maidment ADA. Analysis of Percent Density Estimates from Digital Breast Tomosynthesis Projection Images. Paper presented at: Medical Imaging: Computer-Aided Diagnosis, 2007; San Diego, CA.
6. Byng JW, Boyd NF, Fishell E, Jong RA, Yaffe MJ. The quantitative analysis of mammographic densities. *Physics in Medicine & Biology*. 1994;39(10):1629-1638.
7. Vachon CM, Sellers TA, Vierkant RA, Wu F-F, Brandt KR. Case-Control Study of Increased Mammographic Breast Density Response to Hormone Replacement Therapy *Cancer Epidemiology, Biomarkers, and Prevention* 2002;11:1382-1388.
8. Khan Q, Kimler B, O'Dea A, Zalles C, Sharma P, Fabian C. Mammographic density does not correlate with Ki-67 expression or cytomorphology in benign breast cells obtained by random periareolar fine needle aspiration from women at high risk for breast cancer. *Breast Cancer Research*. 2006;9:R35.
9. Cerhan JR, Sellers TA, Janney CA, Pankratz VS, Brandt KR, Vachon CM. Prenatal and perinatal correlates of adult mammographic breast density. *Cancer Epidemiology, Biomarkers, and Prevention*. 2005;14(6):1502-1508.
10. Gram IT, Bremnes Y, Lund E, Ursin G, Maskarinec G, Bjurstam N. Percentage density, Wolfe's and Tabár's mammographic patterns. Agreement and association with risk factors for breast cancer. *Breast Cancer Research* 2005;7(5):R854-R861.
11. Sim J, Wright CC. The Kappa Statistics in Reliability Studies: Use, Interpretation, and Sample Size Requirements. *Physical Therapy*. 2005;85(3):257-268.
12. Landis J, Koch G. The measurement of observer agreement for categorical data. *Biometrics*. 1977;33:159-174.
13. Yaffe MJ. Digital Mammography. In: Beutel J, Kundel HL, Van Metter RL, eds. *Handbook of Medical Imaging, Volume 1: Physics and Psychophysics*. Vol PM79: SPIE Press; 2000:365.
14. Ursin G, Hovanessian-Larsen L, Parisky YR, Pike MC, Wu AH. Greatly increased occurrence of breast cancers in areas of mammographically dense tissue. *Breast Cancer Research*. 2005;7:R605-R608.
15. Yaffe M, Boyd N. Mammographic breast density and cancer risk: the radiological view. *Gynecological Endocrinology*. 2005;2005(21 Suppl 1):6-11.
16. Saha PK, Udupa JK, Conant EF, Chakraborty DP, Sullivan D. Breast tissue density quantification via digitized mammograms. *IEEE Transactions on Medical Imaging*. 2001;20(8):792-803.
17. Miller PI, Astley SM. Classification of Breast Tissue by Texture Analysis. *Image and Vision Computing*. 1992;10:277-282.